

# Catalysis Science & Technology

Accepted Manuscript



This is an *Accepted Manuscript*, which has been through the Royal Society of Chemistry peer review process and has been accepted for publication.

*Accepted Manuscripts* are published online shortly after acceptance, before technical editing, formatting and proof reading. Using this free service, authors can make their results available to the community, in citable form, before we publish the edited article. We will replace this *Accepted Manuscript* with the edited and formatted *Advance Article* as soon as it is available.

You can find more information about *Accepted Manuscripts* in the [Information for Authors](#).

Please note that technical editing may introduce minor changes to the text and/or graphics, which may alter content. The journal's standard [Terms & Conditions](#) and the [Ethical guidelines](#) still apply. In no event shall the Royal Society of Chemistry be held responsible for any errors or omissions in this *Accepted Manuscript* or any consequences arising from the use of any information it contains.

## Tandem hydroformylation and hydrogenation of dicyclopentadiene by Co<sub>3</sub>O<sub>4</sub> supported gold nanoparticles

Yubo Ma<sup>1#</sup>, Shaojun Qing<sup>2#</sup>, Zhixian Gao<sup>1,2</sup>, Xamxikamar Mamat<sup>1</sup>, Jing Zhang<sup>4</sup>, Hongyi Li<sup>5</sup>, Wumanjiang Eli<sup>1</sup>, Tianfu Wang<sup>1,3\*</sup>

1. *Xinjiang Technical Institute of Physics & Chemistry, Chinese Academy of Sciences, Urumqi, 830011, China;*

2. *Institute of Coal Chemistry, Chinese Academy of Sciences, Taiyuan, 030001, China.*

3. *Department of Power Engineering, Xinjiang Institute of Engineering, Urumqi, 830011, China*

4. *Department of Chemical and Biological Engineering, Iowa State University, Ames, 50011, USA*

5. *Xinjiang Products Supervision & Inspection Institute of Technology, Urumqi, 830011, China*

Corresponding author: tianfuwang@ms.xjb.ac.cn

# These authors contributed equally

**Abstract:** A co-precipitation method was used to prepare a series of Co<sub>3</sub>O<sub>4</sub> supported gold nanoparticles (Au/Co<sub>3</sub>O<sub>4</sub>), which were subsequently evaluated on their performances for “one-pot” synthesis of tricyclodecanedimethylol (TDDMO) from dicyclopentadiene (DCPD). Characterization methods including FTIR, XPS and TG-DTA were performed on the Au/Co<sub>3</sub>O<sub>4</sub> catalyst during the course of reaction to reveal that three distinct stages of catalysis occurred while the catalyst possessed different physiochemical properties. “One-pot” synthesis of TDDMO was successfully realized with selectivity over 90% under relatively mild reaction conditions of 140-150 °C reaction temperature and 7-9 MPa pressure. Experimental data suggested that the catalytically active species might be a Co(CO)<sub>x</sub>(PPh)<sub>y</sub> complex where the presence of

gold can assist the in-situ reduction of  $\text{Co}_3\text{O}_4$  to metallic cobalt under reaction conditions, thereby increasing the number of active sites. Another role of Au was proposed as facilitating hydrogenation of in-situ formed intermediate aldehyde, diformyltricyclodecanes (DFTD), to produce the final product TDDMO.

**Key words:** DCPD; DFTD; gold nanoparticles; phosphine ligand; hydroformylation

## 1. Introduction

Recently, much research interest has been devoted to utilize tricyclodecanedimethylol (TDDMO) as an important intermediate to produce various high performance plastics<sup>1-4</sup>, for example, TDDMO-derived polyester composites, which are a class of polymers with colorimetric and low viscosity properties. Such polyester materials have found widespread applications in water-based dispersants, paints, lubricants etc. In addition, paints containing TDDMO-derived polyester as an additive could also provide excellent adhesive properties under extreme conditions, such as high/low temperature and acidic/basic environment.

Considering the superior potential of TDDMO-based materials in practical use, a lot of research activities have been focused on the synthesis of TDDMO and could be classified into two categories: 1) two-step approach, DCPD first underwent a hydroformylation reaction step to produce the intermediate di-aldehyde followed by a subsequent, separate hydrogenation step; 2) one-step approach where DCPD was converted to the diol in a “one-pot” manner with di-aldehyde as in-situ formed intermediate. In one study, Evans and co-workers<sup>5</sup> described a method where diformyltricyclodecanes (DFTD) was obtained from hydroformylation of DCPD with cobalt and MgO as the catalyst under 180 atm reaction pressure and 140°C reaction temperature. Then, nickel catalyst was used for the hydrogenation to produce the diol.

However, a low DFTD of 67.4% was achieved in the first step leading to a low overall TDDMO yield. In another study, Evans *et al.*<sup>6</sup> reported a DFTD yield of 98% from DCPD, where a Rh-based catalyst was employed at a reaction temperature of 240 °C. DFTD can be further hydrogenated to produce the TDDMO with a selectivity of over 93%. However, this method is less practically feasible due to the very high reaction temperature. Regarding the “one-step” synthesis, Shibatani and co-workers<sup>7</sup> reported that TDDMO can be directly produced from DCPD. The reaction conditions were: homogeneous Co-based catalyst and phosphine ligand, aliphatic alkane as solvent, reaction temperature of 150-200°C, pressure of 70-150 atm. A TDDMO selectivity over 60% can be achieved at almost complete DCPD conversion. Although this method represents a promising pathway, it is difficult to be adopted in industry because very high reaction pressure is required and the overall yield is moderately low due to the undesired side-reactions, the mono-hydroformylated products monoformyltricyclodecenes(MFTD) and their derivative were formed. Furthermore, homogeneous  $\text{Co}(\text{CO})_x$  formed during reaction is quite toxic and can progressively precipitate during the catalytic process. In view of this challenge, the heterogenization of the homogeneous catalysts has attracted extensive attention, mainly adopting the strategy of supported metallic Co or Co-base complex onto solid matrix such as resins<sup>8,9</sup>, activated carbon<sup>10</sup> or  $\text{SiO}_2$ <sup>11,12</sup>.

Bulk gold was traditionally regarded an “inert” element in catalysis. However, recent discoveries found that gold nanoparticles can catalyze a lot of reactions with superior activity and selectivity<sup>13,14</sup>, especially when they are supported on metal oxides likely due to the presence of metal-support interactions<sup>15-17</sup>. In a recent study, Liu *et al.*<sup>18</sup> reported that  $\text{Co}_3\text{O}_4$  supported gold nanoparticles were effective catalysts for hydroformylation of linear olefins to produce the corresponding linear aldehyde. Metallic Co supported on  $\text{Co}_3\text{O}_4$  was suggested as the catalytically active site. However,

the role of gold nanoparticles during catalysis was not thoroughly investigated. Encouraged by this result, we tried to apply the abovementioned  $\text{Co}_3\text{O}_4$ supported gold nanoparticles in the hydroformylation of DCPD. Unfortunately, no appreciable activity was observed, probably because DCPD activation requires a harsher reaction condition. It is reported that the addition of phosphine ligand to the hydroformylation reaction system can exert a significant promotion effect on the catalysis thus lowering the requirement for high reaction temperature and pressure<sup>19-22</sup>.

In the present work, we explore the use of combined  $\text{Co}_3\text{O}_4$ supported gold nanoparticles and added phosphine ligand system to perform the “one-pot” synthesis of TDDMO from DCPD, as shown in Scheme 1. Interestingly, DCPD conversion can be divided into three distinct reaction phase with the first and third steps being relatively fast and the second one being slow. This system was shown to be effective to completely convert DCPD to the final product TDDMO with an overall yield over 90%, higher than all previously reported systems. In order to understand this phenomenon, characterization techniques including FTIR, XPS and TG-DTA were carried out on catalysts at different stages of reaction. FTIR characterization was performed to analyze the solution mixture at different stages. Combined reaction testing results and catalyst characterizations would suggest the following conclusions: the proposed catalytically active site for the production of di-formylated product may exist as a  $\text{Co}_3\text{O}_4$ supported  $\text{Co}(\text{CO})_x(\text{PPh})_y$  complex. The complex was barely formed in the first stage, and gradually increased in amount in the second stage, finally reached maximum in the third stage during catalysis. Correspondingly, MFTD was obtained as the major product in the first two stages and the final desired product TDDMO was mainly

produced in the third stage. Throughout the course of reaction, almost no bi-formylated product DFTD was observed, suggesting that it rapidly underwent subsequent hydrogenation reaction to form its derivative diol. The role of gold nanoparticles was hypothesized to help reduce outmost cobalt oxide to metallic Co, which is ultimately converted to the active sites for hydroformylation.



Scheme 1 “one-pot” synthesis of TDDMO from DCPD

## 2 Experimental

All chemicals used in this study are of analytic grade and were used as received without further purification.

### 2.1 Catalyst preparation

Au/Co<sub>3</sub>O<sub>4</sub> catalyst was prepared by a co-precipitation method. In brief, 10 g Co(NO<sub>3</sub>)<sub>2</sub>·6H<sub>2</sub>O and 0.6 g HAuCl<sub>4</sub>·3H<sub>2</sub>O were dissolved and mixed in 150 mL distilled water. Then, the resultant solution was added dropwise to 600 mL Na<sub>2</sub>CO<sub>3</sub> solution (0.47 M) under vigorous stirring over ~1 h. The reaction mixture was further stirred for 2 h. After filtration and wash with 150–200 mL of distilled water, the resultant solid was dried at 120 °C for 16 h and calcined at 400 °C in the air for 4 h. Finally, around 3 g of Au/Co<sub>3</sub>O<sub>4</sub> catalyst with 10% Au nominal loading was obtained. Likewise, 5%, 15% and 20% Au/Co<sub>3</sub>O<sub>4</sub> were prepared in a similar manner to 10% Au/Co<sub>3</sub>O<sub>4</sub>.

### 2.2 Catalyst characterization

**ICP-AES:** The loadings of Au were determined using an inductively coupled plasma-atomic emission spectrometry (ICP-AES) (ThermoElemental Company in the USA) by dissolving the samples in aqueous nitric acid.

**Temperature-programmed reduction** A FiNESORB-3010 instrument equipped with a TCD detector was used to perform TPR. In a typical measurement, the catalyst (about 100 mg) was heated under dry air at 383 K for 1 h before analysis. The TPR profile was recorded while heating

the sample from room temperature to 673 K at a ramping rate of 10 K/min under a H<sub>2</sub>/Ar (10% v/v) flow.

**X-ray photoelectron spectroscopy** X-ray photoelectron spectroscopy (XPS) analysis was performed with a VG ESCALAB 210 instrument equipped with an Mg anode and a multi-channel detector. Charge referencing was measured against adventitious carbon (C 1s, 285.0 eV). The surface speciation was determined from the peak areas of the corresponding lines using a Shirley-type background and empirical cross section factors for XPS.

**FTIR:** Fourier transform IR (FT-IR) spectra were obtained using a Nicolet 6700 spectrophotometer. The spectra were acquired by accumulating 64 scans at a resolution of 2 cm<sup>-1</sup> in the range of 400–4000 cm<sup>-1</sup>.

**TG-DTA:** Au/Co<sub>3</sub>O<sub>4</sub> modified with PPh<sub>3</sub> pretreated by syngas under the reaction conditions were subjected to a non-isothermal analysis with a TGA standard equipment (TA Instruments, model DTG-60). Each catalyst sample (approximately 4mg±0.05mg) was heated with a ramping rate of 10 °C/min from room temperature to 600 °C while being weighed under nitrogen at a flow rate of 60 ml/min.

### 2.3 Reaction testing

The hydroformylation reactions were carried out in a 200 mL autoclave reactor with an inserted glass liner. In a typical experiment, DCPD (5g), catalyst(0.3g), PPh<sub>3</sub> (0.3g) and THF(20 mL) were added and mixed. An oil bath on a hotplate was used to control the temperature. The reactor was then purged with syngas (the ratio of H<sub>2</sub> to CO is 1:1) three times and finally pressurized to 6Mpa. The reactor was then heated to desired temperature (140°C) with a stirring rate of 650 rpm. At specified time intervals, an aliquot liquid sample was withdrawn and processed for analysis. The samples were analyzed with a GC equipped with FID detector (Shimazu 2014) where HP-5 was used as the column and a normalization method was used for product quantification. The definitions of DCPD conversion, MFTD, DFTD, and TDDMO selectivity are listed below:

$$\text{DCPD conversion} = \frac{\text{Mol}_{\text{DCPDin}} - \text{Mol}_{\text{DCPDout}}}{\text{Mol}_{\text{DCPDin}}} * 100\%$$

$$\text{MFTD selectivity} = \frac{\text{Mol}_{\text{MFTD}}}{\text{Mol}_{\text{DCPDin}} - \text{Mol}_{\text{DCPDout}}} * 100\%$$

$$\text{DFTD selectivity} = \frac{\text{Mol}_{\text{DFTD}}}{\text{Mol}_{\text{DCPDin}} - \text{Mol}_{\text{DCPDout}}} * 100\%$$

$$\text{TDDMO selectivity} = \frac{\text{Mol}_{\text{TDDMO}}}{\text{Mol}_{\text{DCPDin}} - \text{Mol}_{\text{DCPDout}}} * 100\%$$

$\text{DCPD}_{\text{in}}$  was introduced DCPD in moles,  $\text{DCPD}_{\text{out}}$  was unreacted, remaining DCPD in moles when the sample was taken for analysis.

### 3. Results and discussion

#### 3.1 Effect of catalyst pretreatment method on TDDMO synthesis

Co-precipitation method was used to prepare a series of Au/Co<sub>3</sub>O<sub>4</sub> catalysts. These catalysts were then subjected to various modifications before reaction testing. Figure 1 summarized TDDMO synthesis with PPh<sub>3</sub> as the ligand catalyzed by fresh Au/Co<sub>3</sub>O<sub>4</sub> or pretreated by H<sub>2</sub>, syngas, and syngas plus PPh<sub>3</sub>; P<sub>0</sub> is the initial pressure when the reaction temperature was elevated to 140 °C, while P is the actual pressure at the time when the sample was taken for analysis; P<sub>0</sub>-P is the pressure drop. It can be clearly observed that TDDMO synthesis with fresh Au/Co<sub>3</sub>O<sub>4</sub> catalyst proceeded over three distinct stages: the three stages could be distinguished by the rate of pressure drop, a fast first step, followed by a sluggish second and a faster third one. The major product detected in the first two stages was MFTD while TDDMO was the primary molecule produced in the last stage. H<sub>2</sub>-pretreatment catalyst had a similar DCPD conversion kinetic to the fresh one with the first step being slightly faster. However, for catalyst pretreated by syngas, the reaction was stopped at the end of first stage without further



formation of any TDDMO, probably because syngas exerted a prohibitive effect on the active catalytic species formation. For catalyst pretreated by syngas and  $\text{PPh}_3$ , TDDMO was readily produced at a reaction rate close to those found in the third stages in fresh catalyst or  $\text{H}_2$ -pretreated catalyst. Correlation of different pretreatment methods and reaction kinetic data can lead to the conclusion that certain chemical conditions were required for the molecularly active species to be formed during catalysis, leading to high TDDMO production rate and selectivity. Comparing different compositions of produced chemicals involved in various pretreatments, it is speculated that syngas,  $\text{PPh}_3$  and  $\text{Au}/\text{Co}_3\text{O}_4$  together facilitated the formation of required active sites. In order to probe the chemical nature of such species, further detailed characterizations were needed and will be discussed below.

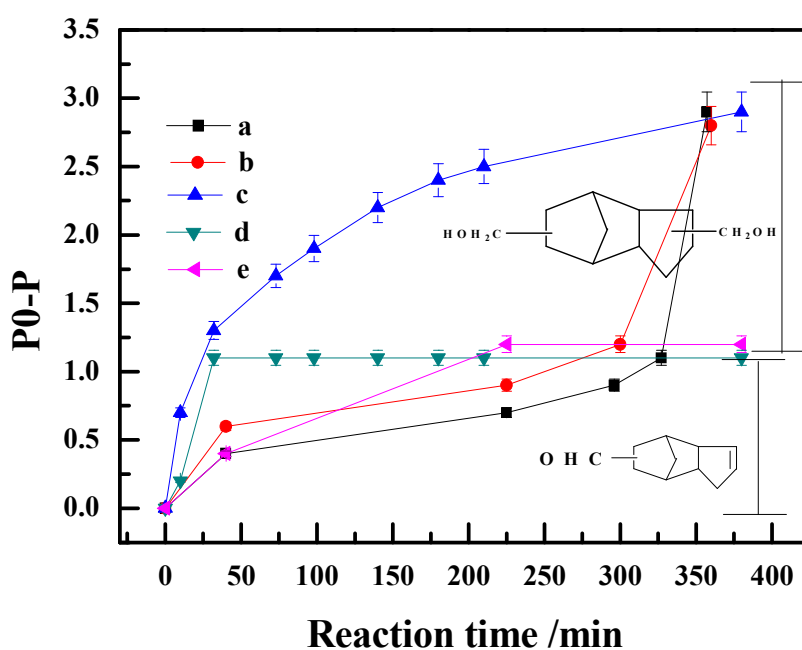


Figure 1. Effect of different catalyst pretreatment method on TDDMO synthesis. Pretreated conditions of  $140^\circ\text{C}$ , 6MPa and 6 h: a) fresh catalyst; b) the catalyst pretreated by  $\text{H}_2$ ; c) the catalyst pretreated by syngas and  $\text{PPh}_3$ ; d) the catalyst pretreated by  $\text{H}_2$  (2nd used); e) the catalyst pretreated by syngas. Reaction conditions: 5 g DCPD; 20 mL THF; 0.3g catalyst;  $140^\circ\text{C}$  reaction temperature; 6MPa reaction pressure; 6 h reaction time

### 3.2 Effect of Au loading on the TDDMO synthesis

It has been reported that Au can promote the spillover of H<sub>2</sub> to form H atom<sup>23-28</sup>. In hydroformylation reaction, no study regarding the effect of Au on reaction activity improvement was conducted, to the best of our knowledge. We hypothesized that for DCPD hydroformylation catalyst Au/Co<sub>3</sub>O<sub>4</sub>, Au can readily convert H<sub>2</sub> to H, thereby enabling the reduction of surface Co<sub>3</sub>O<sub>4</sub> to metallic Co at a lower reaction temperature. Surface Co, PPh<sub>3</sub> and adsorbed CO can form Co(CO)<sub>x</sub>(PPh)<sub>y</sub><sup>3</sup>, which is reported to be the active site for hydroformylation reactions<sup>18, 29, 30</sup>. Au can also function as the hydrogenation catalyst that will ultimately convert the in-situ produce DFTD to the final product TDDMO. The above considerations lead to the speculation that the presence of Au can have a positive role on TDDMO synthesis. Accordingly, different Au/Co<sub>3</sub>O<sub>4</sub> catalysts were prepared with varied Au loading from 5% to 20% and their performances on TDDMO synthesis were shown in Figure 2. As can be seen, TDDMO production rate increases in accordance with the increased Au loading, indicating that the hypothesis of Au participation in catalysis might have occurred. In order to validate this point, complementary spectroscopy studies on catalyst under different reaction stages will be examined in detail.

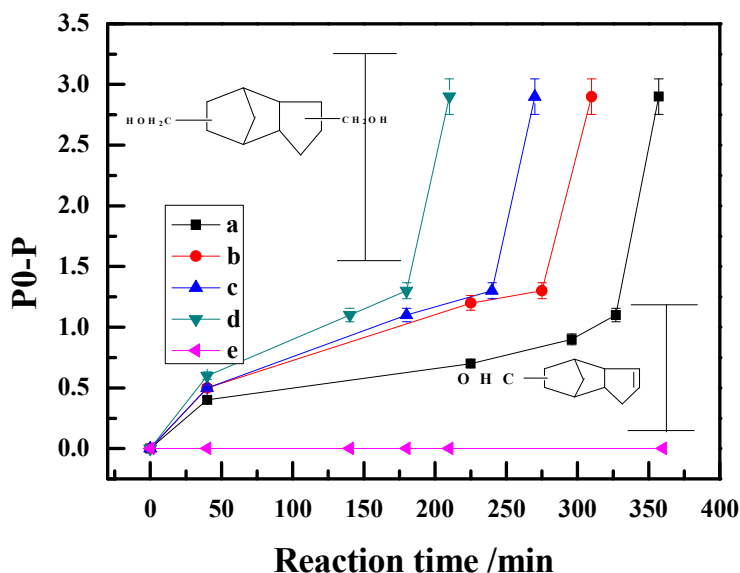


Figure 2. Effect of different Au/Co<sub>3</sub>O<sub>4</sub> loading on TDDMO synthesis Reaction conditions: 5 g DCPD; 20 mL THF; 0.3g catalyst; 0.3 g PPh<sub>3</sub>; 140°C reaction temperature; 6 MPa reaction pressure; 6 h reaction time. a) 5% Au/Co<sub>3</sub>O<sub>4</sub>; b) 10% Au/Co<sub>3</sub>O<sub>4</sub>; c) 15% Au/Co<sub>3</sub>O<sub>4</sub>; d) 20% Au/Co<sub>3</sub>O<sub>4</sub>; e) Co<sub>3</sub>O<sub>4</sub>

### 3.3 Effect of reaction pressure on TDDMO synthesis

Reaction pressure was thought to be an important factor in determining the reaction rate not only because it provided CO and H<sub>2</sub> as the reactants but also CO was hypothesized as an essential component in the formation of the active site Co(CO)<sub>x</sub>(PPh)<sub>y</sub>. As such, the effect of pressure on catalytic performance studies was carried out and the results are plotted in Figure 3. As can be observed, the reaction rates at all three stages of catalysis increased readily with increasing reaction pressure. The pressure of 6 MPa was chosen for further studies because when higher reaction pressure such as 7 MPa was adopted, the pressure plateaued over 10 MPa when the reaction temperature was reached, which will result in safety concerns in practical applications.

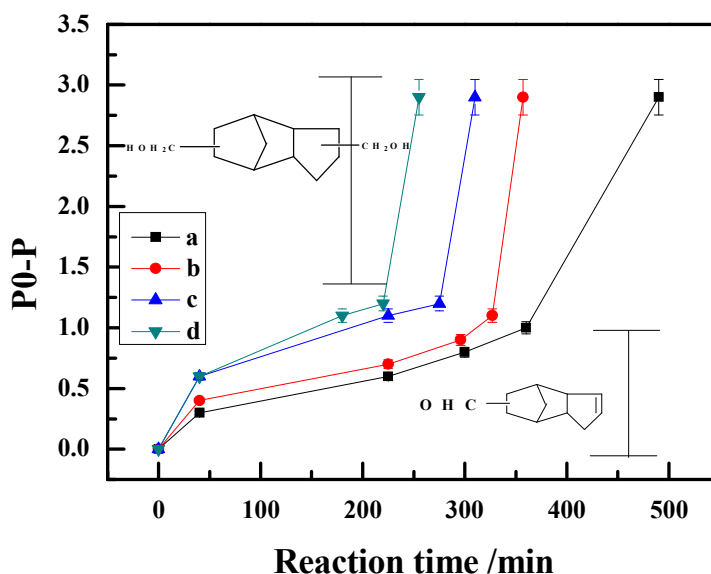


Figure 3. Effect of reaction pressure on TDDMO synthesis.

Reaction conditions: 5 g DCPD; 20 mL THF; 0.3 g 10% Au/Co<sub>3</sub>O<sub>4</sub>; 0.3 g PPh<sub>3</sub>; 140°C reaction temperature; 6 h reaction time. a) 5 MPa reaction pressure; b) 6 MPa reaction pressure; c) 7 MPa reaction pressure; d) 8 MPa reaction pressure;

### 3.4 Catalyst reusability and their activities

Catalyst reusability is of practical importance in industrial deployment of chemical processes. Due to the heterogeneity of currently studied catalyst system, we explored

different recycle method and their effects on the TDDMO synthesis. As shown in Figure 4, for fresh catalyst, a similar three-staged catalysis was observed as compared to results shown in Figure 3. In the first experiment, the supernatant was decanted and collected after the reaction. The mother liquor was combined with freshly added reactant, DCPD and were subjected to reaction conditions. This procedure resulted in the production of mainly MFTD rather than TDDMO. The catalysis occurred probably due to the leaching of some active sites. In the second approach, the recovered solid catalyst was combined with freshly added reactants and solvent. It is found that DCPD was readily converted to the corresponding TDDMO product, without the formation of MFTD intermediate which occurred in the experiment using fresh catalyst. This indicated that an induction period would be required for the fresh catalyst to possess the catalytically active species on the cobalt oxide support.

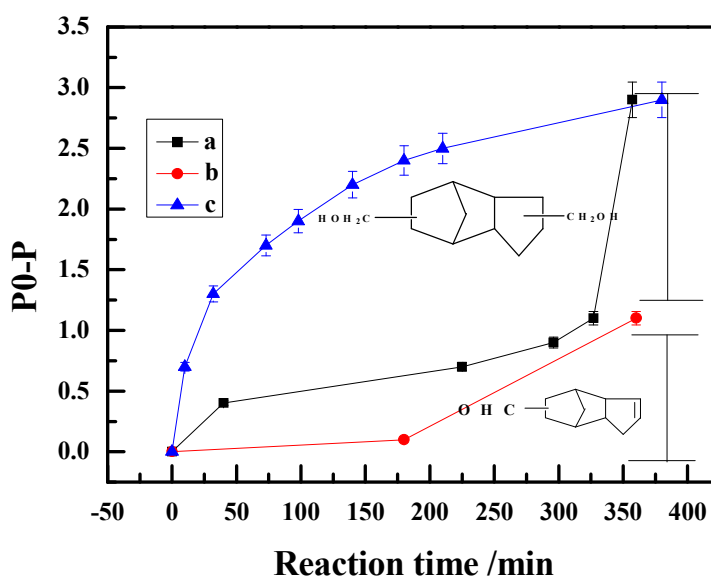


Figure 4. TDDMO synthesis by recycled catalysts

Reaction conditions: 5 g DCPD; 20 mL THF; 0.3g 10% Au/Co<sub>3</sub>O<sub>4</sub>; 0.3 g PPh<sub>3</sub>; 140°C reaction temperature; 6MPa reaction pressure; 6 h reaction time. a) fresh catalyst; b) catalyst reused by removing mother liquid; c) catalyst reused by directly adding DCPD to the autoclave

### 3.5 Reaction mechanism study on TDDMO synthesis

In order to explore the underlying mechanism of the observed three-staged reaction course described in the above sections, catalyst and reaction medium at different stages

were characterized by a set of methods including FTIR, TG-DTA and XPS. 10% Au/Co<sub>3</sub>O<sub>4</sub> catalyst was used all the reactions unless otherwise specified.

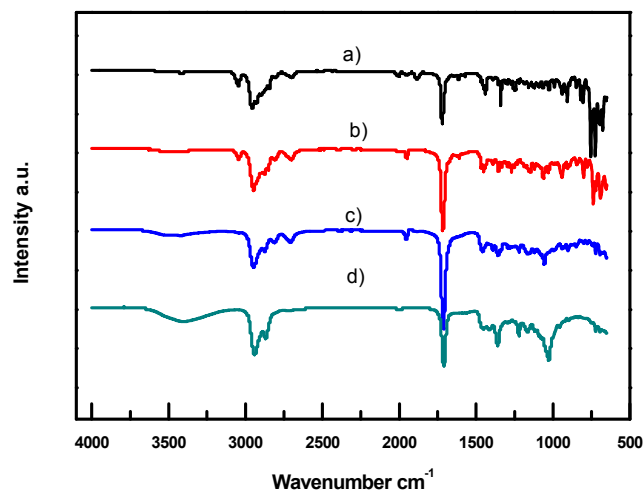


Figure 5. FTIR spectra of liquid medium at different stages of reaction

a) reaction started; b) reaction started for 1 h; c) reaction between first and second stage; d) reaction ended

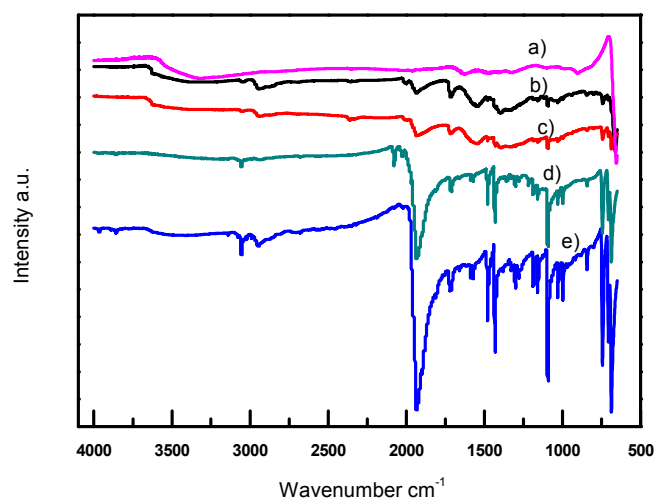


Figure 6. FTIR spectra of Au/Co<sub>3</sub>O<sub>4</sub> catalyst at different reaction stages

a) fresh catalyst; b) catalyst at the beginning of reaction; c) catalyst at the stage of reaction started for 1 h; d) catalyst at the stage of reaction between first and second step; e) catalyst at the end of reaction

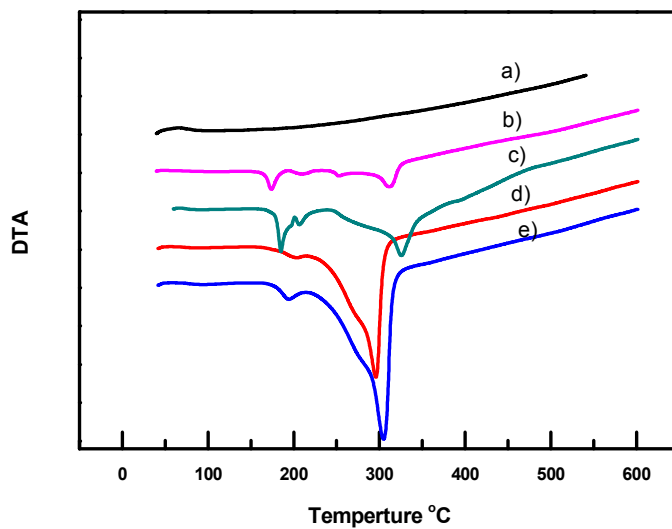


Figure 7. TG-DTA characterization of Au/Co<sub>3</sub>O<sub>4</sub> catalyst at different reaction stages

a) fresh catalyst; b) catalyst at the beginning of reaction; c) catalyst at the stage of reaction started for 1 h; d) catalyst at the stage of reaction between first and second step; e) catalyst at the end of reaction

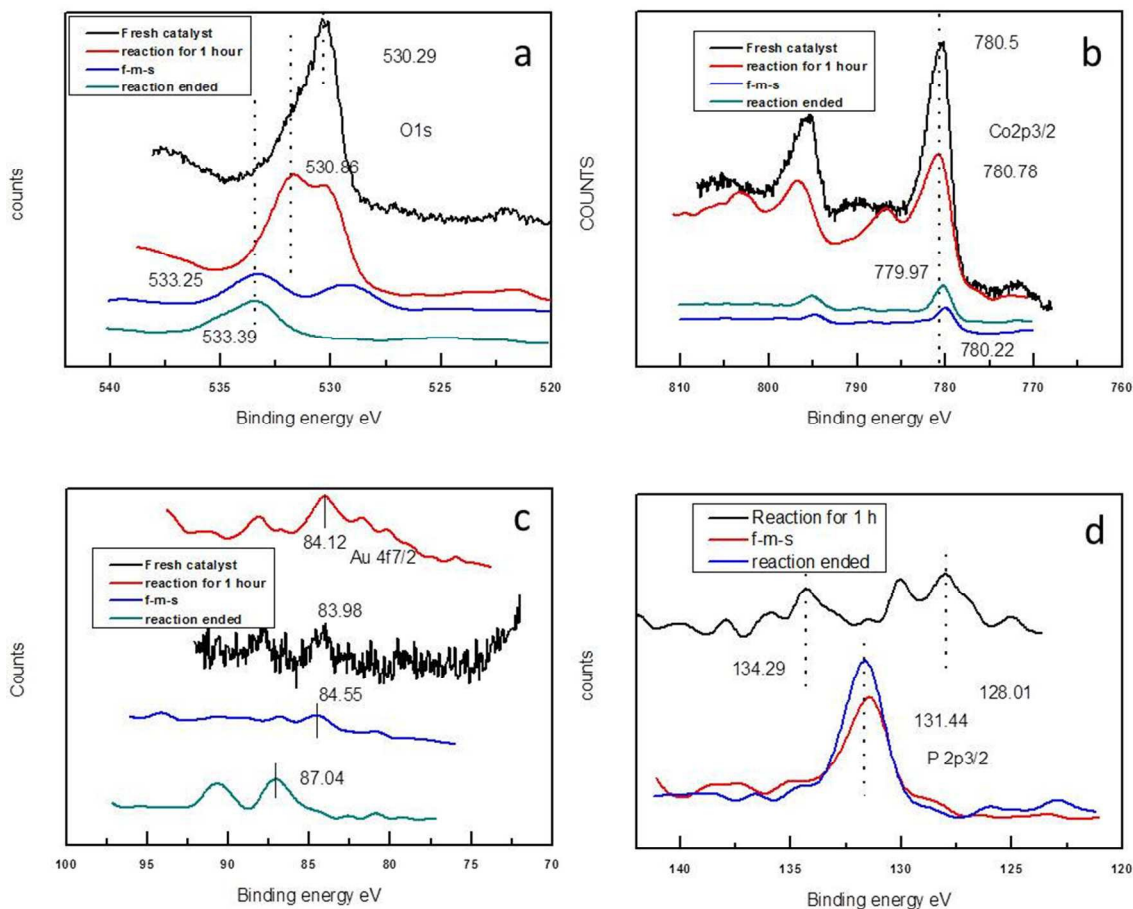


Figure 8. a) XPS of oxygen (O) at different reaction stages; b) XPS of Co at different reaction stages; c) XPS of Au at different reaction stages; d) XPS of P at different reaction stages.

Shown in Figure 5 is the FTIR spectra of reaction medium at different time. Comparing the vibration spectrum leads to the conclusion that the product formed in first and second stages is MFTD while TDDMO is the only product formed after the third stage. FTIR characterization on Au/Co<sub>3</sub>O<sub>4</sub> catalyst at different stages of reaction was also performed and the results are presented in Figure 6. It can be observed that the spectrum was barely changed during the first stage of catalysis compared to fresh catalyst, explaining the very slow rate of DCPD conversion in the first stage was due to the lack of catalytically active sites. Starting from the second stage, several peaks centered at around 1100 cm<sup>-1</sup>, 1500 cm<sup>-1</sup> and 1900 cm<sup>-1</sup> gradually appeared, which was indicative of the formation of Co(CO)<sub>x</sub>(PPh)<sub>y</sub>-type active sites. The strength of these spectra further increased at the end of the third stage of catalysis. Comparing DCPD conversion rate and

the peak strength of catalyst at different stages can verify the positive correlation between them. In addition, TG-DTA was also exploited to confirm the formation of the organic Co complex and the results were plotted in Figure 7. By evaluating the weight loss peaks position and strength, it is found that a small amount of PPh<sub>3</sub> was adsorbed on the Au/Co<sub>3</sub>O<sub>4</sub> catalyst during the first stage and two peaks appeared. As the reaction proceeded, however, significantly greater weight loss peaks were observed for Au/Co<sub>3</sub>O<sub>4</sub> catalyst at the second and third stage. In addition, the center of the peak shifted to around 300°C, which is indicative of a strong chemical interaction such as coordination between PPh<sub>3</sub> and the metal center. FTIR and TG-DTA analysis complementally confirmed the successful formation of the active site Co(CO)<sub>x</sub>(PPh)<sub>y</sub> when the reaction proceeded.

Additionally, XPS characterization over catalyst at different reaction stages was also performed to examine the element speciation of O, Au, Co and P. As shown in Figure 8a-d, Au atom existed in the metallic form, Au(0) throughout the course of reaction. Since XPS is a surface-sensitive technique, the increased peak area implies that Au(0) was slightly enriched near the catalyst surface. Cobalt experienced a drastic change in oxidation status during the reaction course, in accordance with the phase change from Co<sub>3</sub>O<sub>4</sub> to the co-existence of Co<sub>3</sub>O<sub>4</sub> and Co(0) to metallic form, Co(0). The synchronized change in oxygen element XPS data verify the oxidation status change for cobalt. It showed a step change of O from Co<sub>3</sub>O<sub>4</sub> to a mixture of Co<sub>3</sub>O<sub>4</sub> and carbonyl to carbonyl. XPS results for phosphor (P) also complemented the data of the TG-DTA analysis, showing two forms of P existed in the first stage of reaction whereas only one form was seen after the third stage of reaction. All the characterization results above implied that the active sites started to form in the second stage of reaction and maximize in the last stage, leading to faster reaction kinetics. The fast reaction rate associated with reused catalyst also indirectly confirmed this observation.

To further probe the form of existence of the active site on the catalysts for TDDMO synthesis, various pretreatment methods were applied to Au/Co<sub>3</sub>O<sub>4</sub> catalyst before FTIR characterization. As revealed in Figure 9, H<sub>2</sub>-treated catalyst had a superimposable curve with the fresh catalyst, indicating no appreciable organic complex was formed. Cobalt carbonyl was detected in the syngas-treated catalyst sample. Catalyst treated by a combination of syngas and PPh<sub>3</sub>, however, had an identical infrared spectrum feature



with the catalyst after reaction. Comparison of these spectra can lead to the conclusion that the active site would not be  $\text{Co}_3\text{O}_4$ -supported metallic Co ( $\text{H}_2$ -treated sample), nor  $\text{Co}(\text{CO})_n$  (syngas-treated sample), but rather the  $\text{Co}_3\text{O}_4$ -supported  $\text{Co}(\text{CO})_x(\text{PPh})_y$  species. The catalytic activities of these pretreated samples were also evaluated. DCPD conversion reaction by  $\text{H}_2$ -treated catalyst proceeded similarly to the fresh catalyst; however no appreciable activity was observed when the catalyst was reused. Syngas-treated catalyst can transform DCPD to form MFTD but no diol was produced. Syngas and  $\text{PPh}_3$  pretreatment method resulted in catalyst which can effectively produce TDDMO in high yields and could be recycled.

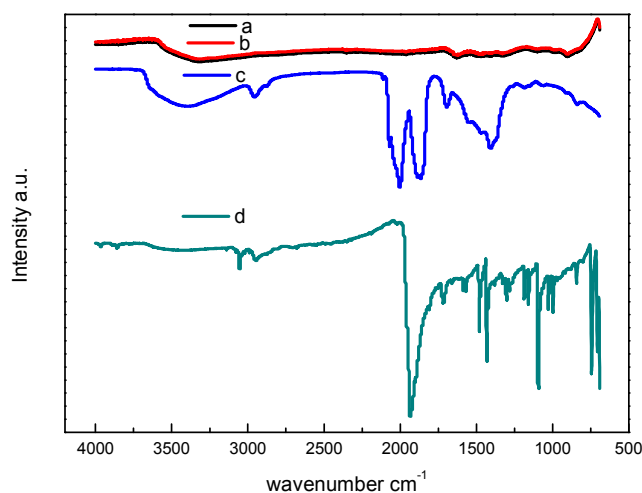


Figure 9. FTIR spectrum of  $\text{Au}/\text{Co}_3\text{O}_4$  after different pretreatment method

- a) fresh catalyst; b) the catalyst pretreated by  $\text{H}_2$ ; c) the catalyst pretreated by syngas;
- d) the catalyst pretreated by syngas and  $\text{PPh}_3$

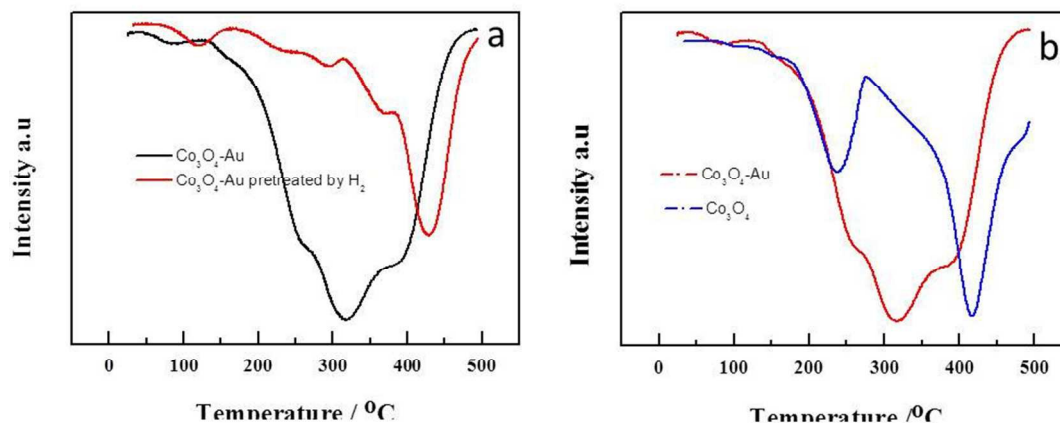


Figure 10.a) TPR profile of Au/Co<sub>3</sub>O<sub>4</sub> with/without H<sub>2</sub> pretreatment; b)TPR profile of Au/Co<sub>3</sub>O<sub>4</sub> and parent Co<sub>3</sub>O<sub>4</sub>

TPR was also exploited as a method to characterize pretreated catalyst samples. Shown in Figure 10a is the TPR profile of Au/Co<sub>3</sub>O<sub>4</sub> sample with and without H<sub>2</sub> reduction. The H<sub>2</sub>-treated sample requires a much higher temperature for the reduction to occur, likely due to the formation of some less reducible cobalt oxide species. Because reduced, metallic cobalt would be required for the formation of active site, the TPR profile can explain why H<sub>2</sub>-treated sample cannot be reused. As can be seen in Figure 10b, lower temperature is required for cobalt oxide to be reduced in the Au/Co<sub>3</sub>O<sub>4</sub> sample compared to the parent Co<sub>3</sub>O<sub>4</sub>. The role of Au in the hydroformylation step can be speculated to help in-situ reduction of cobalt oxide at a lower temperature, leading to the formation of ultrafine metallic Co and subsequent Co-based complex as the catalytically active site. Earlier evaluation on the effect of Au loading can also support the hypothesis because of the positive correlation between Au loading and reaction rate.

Transmission electron microscopy (TEM) was also conducted on both fresh and spent Au/Co<sub>3</sub>O<sub>4</sub> catalyst samples to examine the morphological change of catalyst during catalysis. TEM images in Figure 11 reveal that the co-precipitation method yielded in the formation of Au nanoparticles with spherical shape and diameters of about 8-10 nm. After the reaction, the spent catalyst was also examined to see if any sintering of Au nanoparticles occurred. And from the images of spent catalyst, no obvious sintering was observed, with Au nanoparticles having mean diameters around 8nm shown in Figure 11b.

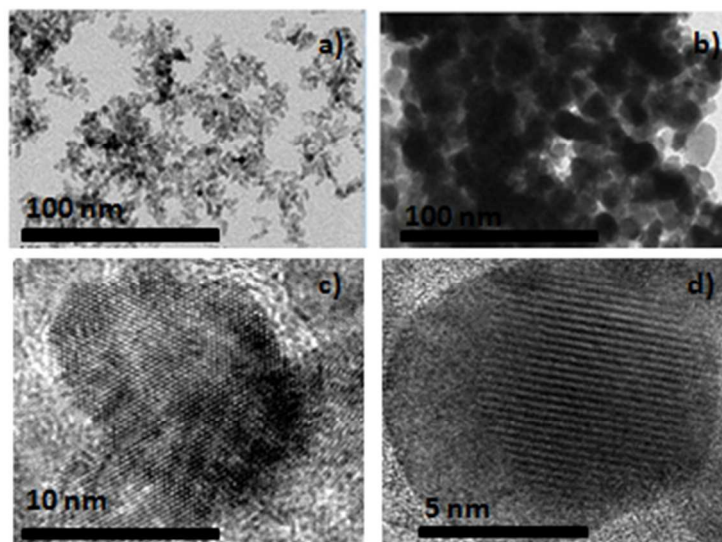


Figure 11. Morphological properties of Au/Co<sub>3</sub>O<sub>4</sub> catalyst. a/c: fresh Au/Co<sub>3</sub>O<sub>4</sub> before reaction; b/d: spent Au/Co<sub>3</sub>O<sub>4</sub> catalyst

Nitrogen adsorption/desorption was also performed on parent Co<sub>3</sub>O<sub>4</sub> support and Au/Co<sub>3</sub>O<sub>4</sub> with different Au loading to examine the textural properties of different catalysts. It can be seen in Table 1, while the addition of Au to parent Co<sub>3</sub>O<sub>4</sub> can lower the surface area, values of average pore diameter and pore volume were barely changed. These results showed that Au nanoparticles are likely well-dispersed on the matrix.

Table.1 Typical physicochemical properties of different catalysts

Sample	Surface area/m <sup>2</sup> /g	Average pore diameter	Pore volume /cm <sup>3</sup> /g
Co <sub>3</sub> O <sub>4</sub>	89	9.6	0.297
5 wt% Au/Co <sub>3</sub> O <sub>4</sub>	58	9.3	0.284
10 wt% Au/Co <sub>3</sub> O <sub>4</sub>	56	9.3	0.279
20 wt% Au/Co <sub>3</sub> O <sub>4</sub>	53	9.2	0.274

In order to prove the proposed synergetic effect between Au nanoparticles and Co<sub>3</sub>O<sub>4</sub> more convincingly, we prepared three different catalysts-10 wt%Co<sub>3</sub>O<sub>4</sub>/SiO<sub>2</sub>, 10 wt% Au/SiO<sub>2</sub> and 10%Au-10%Co<sub>3</sub>O<sub>4</sub>/SiO<sub>2</sub>, by the deposition-precipitation. Hydrogenation of DFTD was tested with these three catalysts and the results were listed in table 2 (entries 1-3). It can be seen that 98% TDDMO selectivity could be achieved over 10wt% Au-10wt%Co<sub>3</sub>O<sub>4</sub>/SiO<sub>2</sub> catalyst at a DFTD conversion of 90%. However,

no activity was observed for either 10 wt%Co<sub>3</sub>O<sub>4</sub>/SiO<sub>2</sub> or 10 wt% Au/SiO<sub>2</sub> catalyst, suggesting that there is a synergetic effect between Au nanoparticles and Co<sub>3</sub>O<sub>4</sub> for the reaction. Additionally, hydroformylation of DCPD was also carried out over these three catalysts, and the results were also listed in table 2 (entries 4-6). As shown in entry 6, 31% MFTD selectivity, 28% DFTD selectivity and 41% TDDMO selectivity could be obtained with 10 wt%Au-10 wt%Co<sub>3</sub>O<sub>4</sub>/SiO<sub>2</sub> as the catalyst, and no activity has been observed over other two catalysts.

Table.2 the results of DCPD hydroformylation and DFTD hydrogenation over 10 wt%Co<sub>3</sub>O<sub>4</sub>/SiO<sub>2</sub>, 10 wt% Au/SiO<sub>2</sub> and 10%Au-10%Co<sub>3</sub>O<sub>4</sub>/SiO<sub>2</sub> catalyst

Entry	Catalyst	Substrate	Conversion %	MFTD selectivity %	DFTD selectivity %	TDDMO selectivity %
1	10 wt% Co <sub>3</sub> O <sub>4</sub> /SiO <sub>2</sub>	DFTD	0	-	-	-
2	10 wt% Au/SiO <sub>2</sub>	DFTD	0	-	-	-
3	10 wt% Au-10 wt% Co <sub>3</sub> O <sub>4</sub> /SiO <sub>2</sub>	DFTD	90	-	-	98
4	10 wt% Co <sub>3</sub> O <sub>4</sub> /SiO <sub>2</sub>	DCPD	0	-	-	-
5	10 wt% Au/SiO <sub>2</sub>	DCPD	0	-	-	-
6	10 wt% Au-10 wt% Co <sub>3</sub> O <sub>4</sub> /SiO <sub>2</sub>	DCPD	100	31	28	41

Reaction conditions: 140 °C reaction temperature; 10 h reaction time; 5 g substrate; 0.6 g catalyst; 0.6 g PPh<sub>3</sub> as the ligand for DCPD hydroformylation.

#### 4. Conclusions

Co-precipitation method was used to synthesize 4 different types of Au/Co<sub>3</sub>O<sub>4</sub> catalysts, which were subsequently applied in the synthesis of TDDMO from DCPD via tandem hydroformylation and hydrogenation process. Experimental results provide evidence that as the Au loading increases, the reaction rate improved substantially. Also, the course of reaction can be divided into three distinct stages. These include a slow first stage where the catalyst is barely altered and MFTD was produced as the major product. Although the catalyst evolved and was gradually transformed to its active form, reaction

rate only slightly increased in the second stage with MFTD being formed as the major product. However, much faster reaction rate was observed in the third stage of reaction, yielding the desired product TDDMO in high selectivity. Various catalyst characterization methods including FTIR, TG-DTA, TPD, TEM in conjunction with reaction rates and model compound adsorption studies complementally confirmed the formation of  $\text{Co}(\text{CO})_x(\text{PPh})_y$  as the catalytically active species.

Au nanoparticles were found to play an important role in the catalytic conversion of DCPD to TDDMO. In the first hydroformylation step, the presence of Au can readily reduce the near-surface  $\text{Co}_3\text{O}_4$  to metallic Co, which ultimately can combine with CO, and  $\text{PPh}_3$  to form the  $\text{Co}(\text{CO})_x(\text{PPh})_y$ , catalyzing the transformation of DCPD to DFTD. In addition, the presence of Au nanoparticles could also facilitate the hydrogenation of in-situ produced DFTD rapidly to the desired product, TDDMO.

In summary, the heterogeneous catalyst system comprising of Au/ $\text{Co}_3\text{O}_4$  and added  $\text{PPh}_3$  could effectively carry out the tandem hydroformylation/hydrogenation of DCPD to TDDMO. A variety of characterization on the catalyst provided in-depth understanding on the catalyst evolution and reaction mechanism, which can be speculated to find applications in other olefin-related conversions for value added fine chemical synthesis.

### Acknowledgments

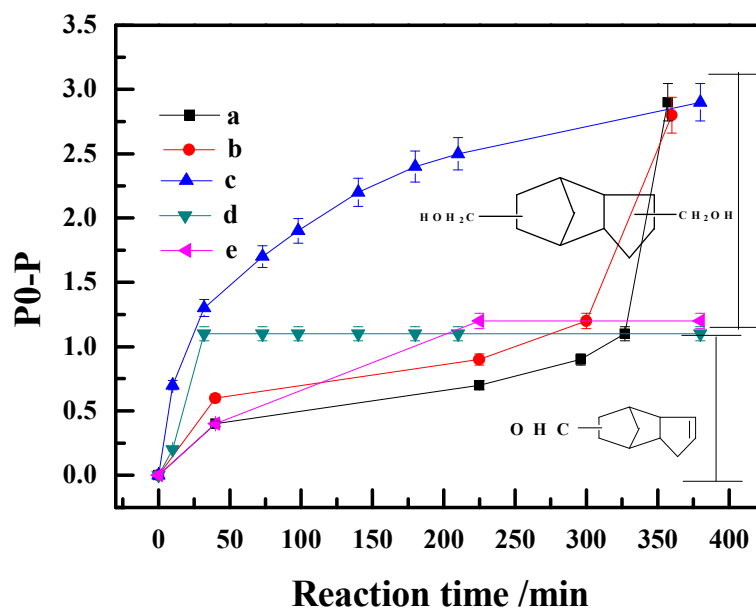
This work has been financially supported by Chinese Government “Thousand Talent” Program (Y42H291501), National Natural Science Foundation of China (U1139302, U1403192), Chinese Academy of Sciences (2015RC013, XBBS201114) and Urumqi Science & Technology Bureau (Y121120006).

### Reference

1. K. Aigami, Y. Inamoto, N. Takaishi, Y. Fujikura, A. Takatsuki and G. Tamura, *Journal of Medicinal Chemistry*, 1976, **19**, 536-540.
2. M. B. Samuel, Richard Pethrick, *US Patent*, 1961, 3005775.
3. M. M. L. Garlaschelli, M.C. Iapalucci, G. Longoni, *Journal of Molecular Catalysis*, 1991, **68**, 7-21.
4. X. Pi, Y. Zhou, L. Zhou, M. Yuan, R. Li, H. Fu and H. Chen, *Chinese Journal of Catalysis*, 2011, **32**, 566-571.
5. E. Edward, *GB patent*, 1952, 750144.
6. E. Edward, *GB patent*, 1969, 1170226.

7. H. S. Y. Ogomori, *US Patent*, 1981, 4300002.
8. F. Shi, Q. Zhang, Y. Ma, Y. He and Y. Deng, *Journal of the American Chemical Society*, 2005, **127**, 4182-4183.
9. F. Shibahara, K. Nozaki and T. Hiyama, *Journal of the American Chemical Society*, 2003, **125**, 8555-8560.
10. B. Li, X. Li, K. Asami and K. Fujimoto, *Energy & Fuels*, 2003, **17**, 810-816.
11. X. Qiu, N. Tsubaki, S. Sun and K. Fujimoto, *Catalysis Communications*, 2001, **2**, 75-80.
12. Y. Zhang, K. Nagasaka, X. Qiu and N. Tsubaki, *Catalysis Today*, 2005, **104**, 48-54.
13. A. S. K. Hashmi, *Chemical Reviews*, 2007, **107**, 3180-3211.
14. A. S. K. Hashmi and G. J. Hutchings, *Angewandte Chemie International Edition*, 2006, **45**, 7896-7936.
15. J. K. Edwards, B. E. Solsona, P. Landon, A. F. Carley, A. Herzing, C. J. Kiely and G. J. Hutchings, *Journal of Catalysis*, 2005, **236**, 69-79.
16. D. Andreeva, V. Idakiev, T. Tabakova and A. Andreev, *Journal of Catalysis*, 1996, **158**, 354-355.
17. T. Hayashi, K. Tanaka and M. Haruta, *Journal of Catalysis*, 1998, **178**, 566-575.
18. X. Liu, B. Hu, K. Fujimoto, M. Haruta and M. Tokunaga, *Applied Catalysis B: Environmental*, 2009, **92**, 411-421.
19. L. Yan, Y. Ding, J. Liu, H. Zhu and L. Lin, *Chinese Journal of Catalysis*, 2011, **32**, 31-35.
20. C. F. R. P.W.N.M. Van Leeuwen, *Journal of Molecular Catalysis*, 1985, **31**, 345-353.
21. R. Luo, H.-r. Liang, X.-l. Zheng, H.-y. Fu, M.-l. Yuan, R.-x. Li and H. Chen, *Catalysis Communications*, 2014, **50**, 29-33.
22. O. Saidi, S. Liu and J. Xiao, *Journal of Molecular Catalysis A: Chemical*, 2009, **305**, 130-134.
23. N. Pasupulety, H. Driss, Y. A. Alhamed, A. A. Alzahrani, M. A. Daous and L. Petrov, *Applied Catalysis A: General*, In press.
24. S. Zhao, X. Tian, J. Liu, Y. Ren and J. Wang, *Computational and Theoretical Chemistry*, 2015, **1055**, 1-7.
25. K. Yang, Y. Li, K. Huang, X. Chen, X. Fu and W. Dai, *International Journal of Hydrogen Energy*, 2014, **39**, 18312-18325.
26. D. A. Panayotov, S. P. Burrows, J. T. Yates and J. R. Morris, *The Journal of Physical Chemistry C*, 2011, **115**, 22400-22408.
27. Y.-W. Chen, H.-J. Chen and D.-S. Lee, *Journal of Molecular Catalysis A: Chemical*, 2012, **363-364**, 470-480.
28. D. A. Panayotov and J. T. Yates, *The Journal of Physical Chemistry C*, 2007, **111**, 2959-2964.
29. H. Mistry, R. Reske, Z. Zeng, Z.-J. Zhao, J. Greeley, P. Strasser and B. R. Cuenya, *Journal of the American Chemical Society*, 2014, **136**, 16473-16476.
30. Y. Yamane, X. Liu, A. Hamasaki, T. Ishida, M. Haruta, T. Yokoyama and M. Tokunaga, *Organic Letters*, 2009, **11**, 5162-5165.

Table of content



## Highlights

- One-pot synthesis of high-value monomer tricyclodecanedimethylol (TDDMO) directly from dicyclopentadiene (DCPD) by  $\text{Co}_3\text{O}_4$  supported gold nanoparticles